



Density functional theory model of amorphous zinc oxide (a-ZnO) and a- $X_{0.375}Z_{0.625}O$ (X= Al, Ga and In)



Anup Pandey^{a,*}, Heath Scherich^b, D.A. Drabold^b

^aDepartment of Physics and Astronomy, Condensed Matter and Surface Science Program, Ohio University, Athens OH 45701, USA

^bDepartment of Physics and Astronomy, Ohio University, Athens OH 45701, USA

ARTICLE INFO

Article history:

Received 24 August 2016

Received in revised form 19 October 2016

Accepted 24 October 2016

Available online 14 November 2016

Keywords:

Amorphous zinc oxide

Doping

EDOS

DFT

ABSTRACT

Density functional theory calculations are carried out to study the topological and electronic structure of amorphous zinc oxide (a-ZnO). The models are chemically ordered with some coordination defects. Models of a- $X_{0.375}Z_{0.625}O$ (X= Al, Ga and In) were also prepared by the “melt-quench” method using the density functional theory calculations. The trivalent dopants reduce the four-fold Zn and O, thereby introducing some coordination defects in the network. The dopants prefer to bond with O atoms. The network topology is discussed in detail. Dopants reduce the optical gap in the density of states by producing defect states while maintaining the extended nature of the conduction band edge.

© 2016 Elsevier B.V. All rights reserved.

1. Introduction

Crystalline ZnO has important applications as a piezoelectric material and because of its property of being transparent in visible light [1]. It has a wide direct band gap (~ 3.37 eV at 300 K) which makes it a promising candidate for optoelectronic devices [1,2]. Therefore, there has been a wealth of experimental work on crystalline ZnO. On the other hand, the study of amorphous ZnO is still in its nascent stage compared to its crystalline counterpart.

The amorphous transparent oxide materials have immense use in device technology [3]. Ionic amorphous oxide semiconductors like a-ZnO have high electron mobility ($\sim 5\text{--}40$ cm²/V s) compared to the covalent amorphous semiconductor like a-Si (~ 1 cm²/V s) which make them a better candidate for device applications such as thin film transistors (TFTs) [4]. Experimentally, various techniques such as pulse laser deposition [5], molecular beam epitaxy [6], radio-frequency magnetron sputtering [7] etc. have been used to make a-ZnO and the structure obtained is highly dependent on the substrate material and temperature. There are advantages of a-ZnO over its crystalline counterpart. First, it is easier and more cost efficient to produce a large amorphous sheet compared to a large single crystal. Also, the a-ZnO has been prepared at low temperature (~ 300 K) compared to crystalline ZnO (~ 800 K– 1100 K) [1]. On doping trivalent

elements such as Al, Ga and In on a-ZnO mobility can be increased significantly [8].

In this work, we report the structure and electronic properties of amorphous phases of ZnO and a-ZnO doped with trivalent dopant atoms such as Indium (In), Gallium (Ga) and Aluminium (Al) using a plane wave basis density functional theory (DFT) code and comparisons with the experiments and other molecular dynamics (MD) simulations are made when possible. For the first time, accurate methods are used to compute the topological and chemical order of the materials and determine the electronic properties.

The paper is arranged as follows. In Section 2, we provide details about the computational technique used in modeling various models. In Section 3, we present the simulation results for a-ZnO and a- $X_{0.375}Z_{0.625}O$ (X= Al, Ga and In) and make comparisons with experiments and other MD methods.

2. Computational methods

Density functional theory (DFT) calculations are performed using the plane-wave basis code VASP [10–12], using projected augmented plane waves (PAW) [13] with the Perdew-Burke-Ernzerhof (PBE) exchange-correlation functional [14] and a plane-wave cutoff off energy of 300 eV. All calculations were carried out at Γ point. For a-ZnO, the system consists of 128 atoms in a cubic box of side 12.34 Å corresponding to the experimental density of 4.6 g/cm³ [2]. A random initial configuration is equilibrated at 5000 K, is then cooled to 3000 K at 100 K/ps followed by an equilibration of 5 ps. The

* Corresponding author.

structure at 3000 K is cooled in steps to temperatures 2300 K, 1600 K and 300 K at the rate of 50 K/ps followed by 5 ps equilibration at each temperature. Finally, the structure at 300 K is quenched to 0 K at the rate of 25 K/ps which is again followed by equilibration of 5 ps. The structure is then relaxed using the conjugate gradient (CG) method. This model is termed Model 1. To contrast different quench rates, the configuration at 3000 K was also cooled to 300 K at a rate of 180 K/ps followed by the equilibration of 5 ps. Finally, the equilibrated structure is quenched to 0 K at a rate of 50 K/ps and then equilibrated for another 5 ps. The model is relaxed using CG method. We call this Model 2.

For $a\text{-}X_{0.375}Zn_{0.625}O$ ($X = \text{Al, Ga and In}$), a random starting configuration of 128 atoms was melted at 5000 K followed by cooling to 3000 K at 100 K/ps and then equilibrated for 5 ps. A subsequent schedule of cooling is carried out at temperatures 2300 K, 1600 K and 300 K at a rate of 25 K/ps followed by the equilibration of 5 ps in each temperature. Finally, the structures are cooled to 0 K at the rate of 40 K/ps followed by an equilibration of 5 ps. The final structures are volume relaxed with the conjugate gradient method to tune the density. The cubical box lengths for Al-, Ga- and In-doped models after volume relaxations are 12.26 Å, 12.28 Å and 12.31 Å respectively, close to the assumed 12.34 Å.

3. Results

3.1. Amorphous zinc oxide ($a\text{-}ZnO$)

Structural properties are investigated by the radial distribution functions (RDFs) and partial radial distribution functions. The total RDFs for Model 1 and Model 2 are shown in Fig. 1. The partial pair correlation functions for Zn-Zn, Zn-O and O-O are shown in Fig. 2. The partials for both models show similar features. For both Zn-Zn and O-O partials, the first peak is around 3.30 Å while for Zn-O the first peak position is at 2.00 Å as shown in Fig. 2.

The network is chemically ordered. We calculated the coordination number for Zn and O. Most of the atoms are four-fold coordinated with above 75% four-fold coordinated Zn and O in both the models. Our models exhibit a higher fraction of four-fold Zn compared to the empirical molecular dynamics simulation model (~60%) [2]. The average coordination number for Zn (n_{Zn}) and O (n_O) and the 3-, 4- and 5-fold coordinated Zn and O, denoted by the respective subscript (Zn_3, O_3, \dots) is shown in Table 1. The DFT energy per atom for Model 1 is -4.36 eV/atom and for Model 2 is -4.34 eV/atom (Table 1). The energies of the two models are comparable.

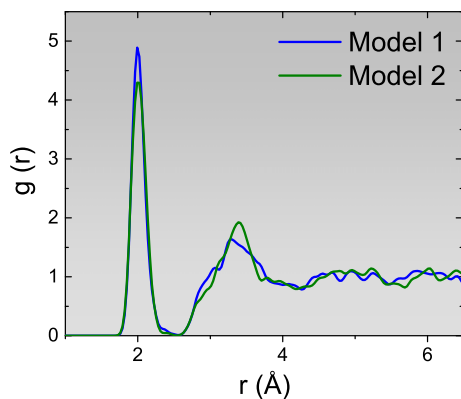


Fig. 1. The total radial distribution function (RDF) for $a\text{-}ZnO$ models. Model 1 and Model 2 correspond to the models obtained by two different quenching rates as described in the Computational methods section. Blue is for Model 1 and green is for Model 2.

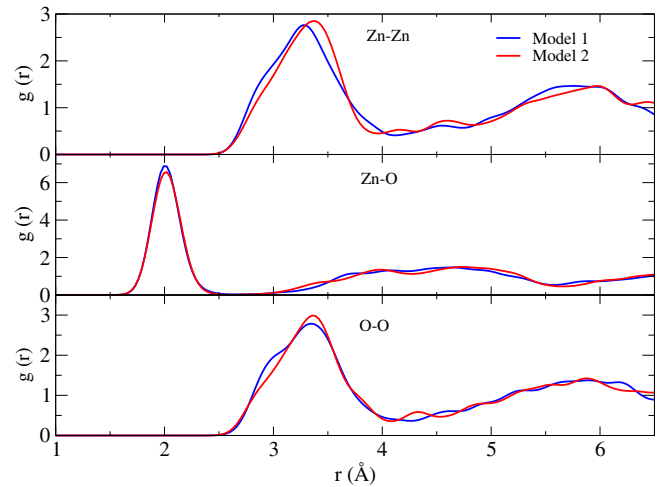


Fig. 2. Partial pair correlation functions for 128-atom models of $a\text{-}ZnO$. Blue is for Model 1 and red is for Model 2 as described in the Computational methods section.

The electronic structure is analysed by calculating the electronic density of states (EDOS) and inverse participation ratio (IPR) of the individual states. The EDOS is just taken to be the density of Kohn-Sham eigenvalues and the IPR is computed from the atom-projected Kohn-Sham eigenvectors. The EDOS is shown in Fig. 3 (black) and the green vertical lines represents the electronic state localization measured by IPR [15,16]. The value of IPR is 1 for a highly localized state and $1/N$ for an extended state, where N is the number of atoms. IPR in Fig. 3 shows that the localization of valence tail states is much larger than the conduction tail states. Thus, the mobility of n -type of carrier is expected to be much higher than the p -type. This feature supports the asymmetry in the localization of valence and conduction band tail states in amorphous metal oxide by Robertson [4]. Similar asymmetrical behavior in amorphous gallium nitride was shown by Cai and Drabold [17].

The band gap (gap between the highest occupied electronic state and the lowest unoccupied electronic state), is 1.36 eV which is slightly less than the experimental band gap of 1.60 eV between the valence band edge and $Zn4s4p$ states [20]. The band gap is always underestimated in a DFT-GGA calculation which could be improved by using hybrid functional [18], GW approximation [19], etc.

3.2. Al-, Ga- and In-doped amorphous ZnO: $a\text{-}X_{0.375}Zn_{0.625}O$ ($X = \text{Al, Ga and In}$)

To investigate the effect of trivalent dopants on local coordination and electronic structure of $a\text{-}ZnO$, 37.5% of Zn is replaced by

Table 1

Coordination number for Zn and O expressed in percentage, average coordination number and the DFT-GGA energy for $a\text{-}ZnO$ model. The coordination numbers for Zn are compared with the other MD model [2]. As expected there are a few more coordination defects in the more rapidly quenched model 2.

	Model 1	Model 2	MD (Ref. [2])
Zn-Zn (%)	0	0	–
O-O (%)	0	0	–
Zn_3 (%)	15.63	23.44	32.00
Zn_4 (%)	81.25	75.00	60.00
Zn_5 (%)	3.12	1.56	7.00
O_3 (%)	15.63	25.00	–
O_4 (%)	81.25	71.88	–
O_5 (%)	3.12	3.12	–
n_{Zn}	3.88	3.78	–
n_O	3.88	3.78	–
Energy (eV/atom)	–4.36	–4.34	–

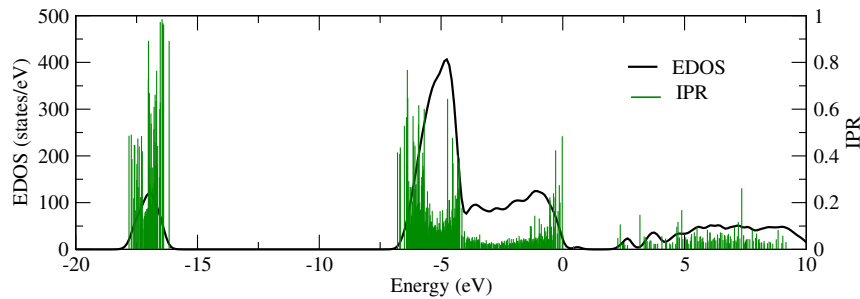


Fig. 3. (black) Electronic density of states of the 128-atom model a-ZnO (Model 1) obtained using GGA-PBE density functional theory calculation. The green vertical lines represent the inverse participation ratio (IPR) used to measure the electronic state localization. Longer IPR implies strong localization. The Fermi level is at 0.28 eV. The PBE gap is 1.36 eV.

group III elements X (X = Al, Ga and In) to model $a\text{-X}_{0.375}\text{Zn}_{0.625}\text{O}$. The atomic percentage of dopants in all the models is 18.75%. The effect of dopants on structure and electronic properties are investigated by RDFs, partial pair correlation functions and electronic density of states.

The total RDFs for In-doped a-ZnO is shown in Fig. 4a. The Zn-O correlation is not affected by the presence of dopants while there is a slight decrease in the correlation peaks for Zn-Zn

and O-O which is illustrated in Table 2. The peak positions are obtained from the partial pair correlation functions shown in Fig. 4b for In-doped a-ZnO and similar plots for Al-, and Ga-doped a-ZnO which is not shown here. The 4-fold Zn and O are reduced significantly in all three doped models. The Al and In bond only with O. In the Al-doped model, 95.83% and 4.17% Al forms 4-fold and 3-fold bond with O. In the In-doped model, 20.83%, 25.00%, 8.33%, 37.5% and 8.34% In form 6-, 5-, 4-, 3- and 2-fold bond with O atom. In the Ga-doped model, 58.33% and 33.33% Ga form 4-fold and 3-fold bond with O while 8.34% Ga form 3-fold with O and 1-fold with Zn. This suggests that the group III elements are more likely to form a bond with O while introduced to a-ZnO.

The Zn-Zn and In-In distances in our model are around 3.26 Å and 3.50 Å which is close to 3.20–3.40 Å for Zn-Zn and 3.30–3.6 Å for In-In of classical MD model [21]. This compares well with the average metal-metal peak in X-ray diffraction measurements of IZO thin layers [22]. Also, the Zn-O and In-O distances in our model are around 2.00 Å and 2.20 Å compared to the 1.95 Å – and 2.20 Å respectively of the classical MD model [21]. These peak positions are consistent with the metal-oxygen peaks at 2.12–2–14 Å in the experiment [22].

The electronic density of states (EDOS) for $a\text{-X}_{0.375}\text{Zn}_{0.625}\text{O}$ (X = Al, Ga and In) models is shown in Fig. 5. Dopants lead to the creation of defect states. The localized states near the valence band edge induced by doping can be associated to the increase in undercoordinated O atoms in the network introduced by doping. The conduction band edge is unaltered by the addition of dopant elements. The extended nature of the conduction band is preserved by the addition of dopants which is in accordance with the conclusion by Hosono [8]. On the other hand, in crystalline ZnO doped by group III elements Al, Ga and In, the dopants form extra localized level in the conduction band, which modifies the conduction band and reduces the optical band gap [9].

4. Conclusions

In conclusion, we have created models of amorphous zinc oxide (a-ZnO) using a melt-quench method and studied their structural and electronic properties in detail. The electronic band gap of our

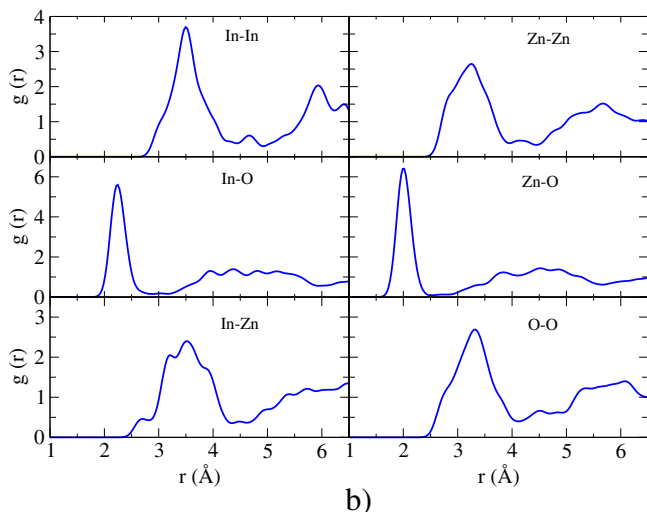
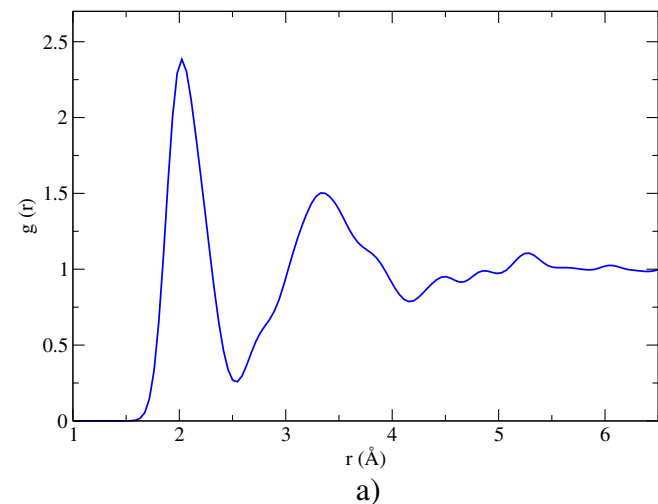


Fig. 4. (a) Total pair correlation functions for 128-atom $\text{In}_{0.375}\text{Zn}_{0.625}\text{O}$ model. (b) Partial pair correlation function of $\text{In}_{0.375}\text{Zn}_{0.625}\text{O}$ model.

Table 2
First peak position for Zn-Zn, Zn-O and O-O partial pair correlation functions of a-ZnO (Model 1) and $a\text{-X}_{0.375}\text{Zn}_{0.625}\text{O}$ (X = Al, Ga and In) models.

	Peak position (Å)			
	ZnO (Model 1)	$\text{Al}_{0.375}\text{Zn}_{0.625}\text{O}$	$\text{Ga}_{0.375}\text{Zn}_{0.625}\text{O}$	$\text{In}_{0.375}\text{Zn}_{0.625}\text{O}$
Zn-Zn	3.28	2.60	2.87	3.26
Zn-O	2.00	2.00	2.00	2.00
O-O	3.36	2.93	3.10	3.33

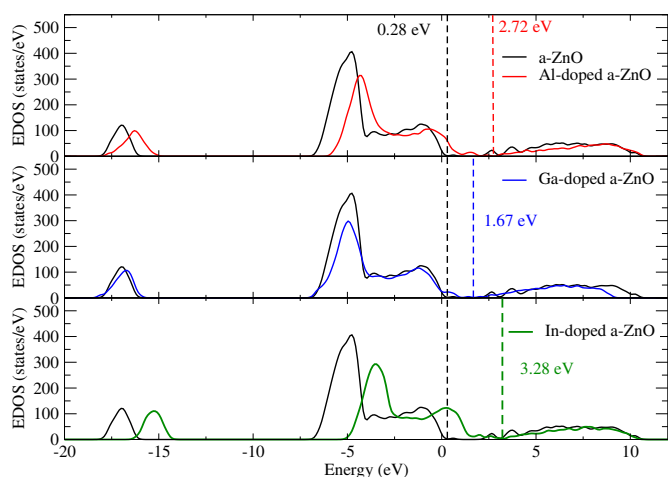


Fig. 5. Electronic density of states for $a\text{-}X_{0.375}Zn_{0.625}O$ ($X = \text{Al, Ga and In}$) models compared to that of $a\text{-}ZnO$. The Fermi levels are shown by vertical broken lines.

model is 1.36 eV which is in reasonable agreement with the experimental band gap 1.60 eV. We have calculated the DFT energies for the two models of $a\text{-}ZnO$ obtained by different quenching rate for comparison. The effect of trivalent dopants in the local structure and the electronic structure of $a\text{-}ZnO$ is investigated in detail by preparing $a\text{-}X_{0.375}Zn_{0.625}O$ ($X = \text{Al, Ga and In}$) models by melt-quench method. The dopants reduce the number of 4-fold coordinated Zn and O in the network and most of them prefer to bond with oxygen. The electronic gap is reduced by the presence of defect states by forming undercoordinated O states in the valence band edge while the conduction band edge is still extended. Coordinates are available upon request.

Acknowledgments

We thank the US NSF under the grants DMR 150683, 1507166 and 1507670 for supporting this work, and the Ohio Supercomputer Center for computer time. We acknowledge the financial support of Condensed Matter and Surface Science program of Ohio University.

References

- [1] J.M. Khoshman, M.E. Kordesch, Optical constants and band edge of amorphous zinc oxide thin films, *Thin Solid Films* 515 (18) (2007) 7393–7399.
- [2] K.H. Lin, S.J. Sun, S.P. Ju, J.Y. Tsai, H.T. Chen, J.Y. Hsieh, Observation of the amorphous zinc oxide recrystalline process by molecular dynamics simulation, *J. Appl. Phys.* 113 (7) (2013) 073512.

- [3] K. Nomura, H. Ohta, A. Takagi, T. Kamiya, M. Hirano, H. Hosono, Room-temperature fabrication of transparent flexible thin-film transistors using amorphous oxide semiconductors, *Nature* 432 (7016) (2004) 488–492.
- [4] J. Robertson, Physics of amorphous conducting oxides, *J. Non-Cryst. Solids* 354 (19) (2008) 2791–2795.
- [5] S. Hayamizu, H. Tabata, H. Tanaka, T. Kawai, Preparation of crystallized zinc oxide films on amorphous glass substrates by pulsed laser deposition, *J. Appl. Phys.* 80 (2) (1996) 787–791.
- [6] D.M. Bagnall, Y.F. Chen, Z. Zhu, T. Yao, S. Koyama, M.Y. Shen, T. Goto, Optically pumped lasing of ZnO at room temperature, *Appl. Phys. Lett.* 70 (17) (1997) 2230–2232.
- [7] Z. Xingwen, L. Yongqiang, L. Ye, L. Yingwei, X. Yiben, Study on ZnO thin films deposited on sol-gel grown ZnO buffer by RF magnetron sputtering, *Vacuum* 81 (4) (2006) 502–506.
- [8] H. Hosono, Ionic amorphous oxide semiconductors: Material design, carrier transport, and device application, *J. Non-Cryst. Solids* 352 (9) (2006) 851–858.
- [9] J.A. Sans, J.F. Sánchez-Royo, A. Segura, G. Tobias, E. Canadell, Chemical effects on the optical band-gap of heavily doped ZnO: M III ($M = \text{Al, Ga, In}$): an investigation by means of photoelectron spectroscopy, optical measurements under pressure, and band structure calculations, *Phys. Rev. B* 79 (19) (2009) 195105.
- [10] G. Kresse, J. Hafner, Ab initio molecular dynamics for liquid metals, *Phys. Rev. B* 47 (1) (1993) 558.
- [11] G. Kresse, J. Furthmüller, Efficient iterative schemes for ab initio total-energy calculations using a plane-wave basis set, *Phys. Rev. B* 54 (16) (1996) 11169.
- [12] G. Kresse, J. Furthmüller, Efficiency of ab-initio total energy calculations for metals and semiconductors using a plane-wave basis set, *Comput. Mater. Sci.* 6 (1) (1996) 15–50.
- [13] G. Kresse, D. Joubert, From ultrasoft pseudopotentials to the projector augmented-wave method, *Phys. Rev. B* 59 (3) (1999) 1758.
- [14] J.P. Perdew, K. Burke, M. Ernzerhof, Generalized gradient approximation made simple, *Phys. Rev. Lett.* 77 (18) (1996) 3865.
- [15] R. Atta-Fynn, P. Biswas, D.A. Drabold, Electron-phonon coupling is large for localized states, *Phys. Rev. B* 69 (24) (2004) 245204.
- [16] K. Prasai, P. Biswas, D.A. Drabold, Electrons and phonons in amorphous semiconductors, *Semicond. Sci. Technol.* 31 (7) (2016) 73002–73015.
- [17] P. Stumm, D.A. Drabold, Can amorphous GaN serve as a useful electronic material? *Phys. Rev. Lett.* 79 (4) (1997) 677.
- [18] J. Heyd, G.E. Scuseria, M. Ernzerhof, Hybrid functionals based on a screened Coulomb potential, *J. Chem. Phys.* 118 (18) (2003) 8207–8215.
- [19] F. Aryasetiawan, O. Gunnarsson, The GW method, *Rep. Prog. Phys.* 61 (3) (1998) 237.
- [20] D. Schmeier, J. Haeberle, P. Barquinha, D. Gaspar, L. Pereira, R. Martins, E. Fortunato, Electronic structure of amorphous ZnO films, *Phys. Status Solidi (C)* 11 (910) (2014) 1476–1480.
- [21] D.M. Ramo, A. Chronos, M.J.D. Rushton, P.D. Bristowe, Effect of trivalent dopants on local coordination and electronic structure in crystalline and amorphous ZnO, *Thin Solid Films* 555 (2014) 117–121.
- [22] T. Eguchi, H. Inoue, A. Masuno, K. Kita, F. Utsuno, Oxygen close-packed structure in amorphous indium zinc oxide thin films, *Inorg. Chem.* 49 (18) (2010) 8298–8304.